CMS Physics Analysis Summary

Contact: cms-pag-conveners-b2g@cern.ch 2016/05/19

Combination of searches for WW, WZ, ZZ, WH, and ZH resonances at $\sqrt{s}$ = 8 and 13 TeV

The CMS Collaboration

Abstract

The statistical combination of searches for massive resonances decaying to pairs of W, Z, and Higgs bosons based on pp collision data collected by the CMS experiment at the CERN LHC is presented. The data are taken at a centre-of-mass energy of 8 and 13 TeV and correspond to an integrated luminosity of 19.7fb^{-1} and 2.6^{-1} respectively. The results are interpreted in the context of a heavy vector triplet model that mimics the properties of composite Higgs models predicting a W′ and a Z′ decaying to WZ, WH, WW, and ZH and a model with a "bulk" graviton that decays into WW and ZZ. Combined cross section limits as a function of resonance mass are obtained. The combined significance of potential resonances of 1.8–2 TeV are evaluated in each signal hypothesis.

1 Introduction

Several theories of physics beyond the standard model (SM), including models of warped extra dimensions [1, 2] and composite Higgs scenarios [3–6], predict the existence of heavy resonances that decay into pairs of heavy SM bosons, namely W, Z bosons (V), and SM-like Higgs bosons (H). In Run 1 and Run 2 of the CERN LHC, searches for such VV and VH resonances in various final states have been performed with the CMS experiment [7–14]. As these searches have very similar sensitivity to benchmark physics scenarios of interest, a statistical combination to maximize the overall sensitivity is performed and presented in this note. A combination of analyses of heavy diboson resonances is of recent interest as searches in the all-hadronic WW/WZ/ZZ [15] and the semileptonic WH [13] channels have shown slight excesses. The combined significance around 2 TeV is therefore presented in various signal hypotheses in this note.

The reference benchmark models considered in the combination are the bulk scenario [16–18] (G_{bulk}) of the Randall–Sundrum Warped Extra Dimensions model [1, 2], a heavy vector triplet (HVT) model [19] (W′ and Z′) as well as vector singlets (W′ or Z′). The HVT generalizes a large number of explicit models predicting spin-1 resonances, such as composite Higgs scenarios. These models are considered as benchmark scenarios for diboson resonances having spin 1 ($W' \to WZ$ or WH, $Z' \to WW$ or ZH) and spin 2 ($G_{bulk} \to WW$ or ZZ), produced via quark-antiquark annihilation ($q\bar{q}' \to W'$, $q\bar{q} \to Z'$) and gluon-gluon fusion ($gg \to G_{bulk}$).

The analyses entering the statistical combination are based on proton-proton collision data collected by the CMS experiment at the LHC during 2012 and 2015 at $\sqrt{s} = 8\,\text{TeV}$ and $13\,\text{TeV}$, corresponding to an integrated luminosity of $19.7\,\text{fb}^{-1}$ and $2.2\text{–}2.6\,\text{fb}^{-1}$ respectively. The signal is a narrow resonance with mass above 0.8 TeV that decays to a pair of highly boosted W, Z, and H bosons. Narrow refers to the assumption that the resonance's natural width is much smaller than the experimental resolution, covering a large fraction of the parameter space of the reference models considered. Analyses with all-leptonic, semi-leptonic, and all-jets final states containing charged leptons (ℓ), neutrinos (ν) from the decay of W and Z bosons, and/or reconstructed jets containing the decay products of hadronically decaying W or Z bosons (labeled as $q\bar{q}$ final states that include $W \to q\bar{q}' \to$ jet and $Z \to q\bar{q} \to$ jet) or Higgs bosons (labeled as $b\bar{b}$ or $q\bar{q}q\bar{q}$ final states referring to $H \to b\bar{b}$ or $H \to q\bar{q}'q\bar{q}'$) are considered. These include the analyses aiming at the final states containing $\ell\nu q\bar{q}$ (13 TeV) [7], $q\bar{q}q\bar{q}$ (13 TeV) [7], $\ell\ell b\bar{b}/\ell\nu b\bar{b}/\nu\nu b\bar{b}$ (13 TeV) [8], $3\ell\nu$ (8 TeV) [12], $\ell\nu q\bar{q}$ (8 TeV) [9], $\ell\ell q\bar{q}$ (8 TeV) [9], $q\bar{q}q\bar{q}$ (8 TeV) [10], $\ell\nu b\bar{b}$ (8 TeV) [13], $q\bar{q}b\bar{b}/q\bar{q}q\bar{q}q\bar{q}$ (8 TeV) [11], $q\bar{q}\tau\tau$ (8 TeV) [14].

As the experimental signature of hadronically decaying W and Z bosons cannot fully be discriminated given the experimental jet mass resolution, analyses can be sensitive to multiple signals predicted by the same model. E.g., $\ell\nu q\bar{q}$ is sensitive to HVT $W' \to WZ$ and $Z' \to WW$. This contribution of multiple signals to the same analysis is therefore taken into account in the combination. For this reason separate interpretations for vector singlets (W′ or Z′) and a vector triplet (W′ and Z′) are presented in this note.

The note is structured as follows. After a short introduction to the benchmark physics models in Section 2, a summary of each analysis entering the combination is given in Section 3. The combination procedure is described in Section 4, and finally the results and conclusions are presented in Section 5 and Section 6.

2 Theory models

Heavy diboson resonances are predicted by a large class of models that attempt to explain the apparently large difference between the electroweak and the gravitational scale. We perform the combination in four different benchmark scenarios of interest covering different spin, production, and decay scenarios for resonances decaying to VV and VH. The physics motivation and properties of models predicting spin-1 and spin-2 resonances are described in the following two sections. At the end of this section, the properties of the described benchmark resonances studied in this note are summarized in Table 1.

2.1 Spin-1 resonances

Heavy Spin-1 resonances are predicted by several extensions of the standard model such as Composite Higgs [3–6] and Little Higgs [20, 21] models, and the Sequential Standard Model (SSM) [22]. These models can be generalized by a phenomenological Lagrangian describing the production and decay of spin-1 heavy resonances, such as charged W' and neutral Z', in the heavy vector triplet (HVT) [19] hypothesis.

The HVT couplings are parametrized in terms of four parameters:

c_H describes interactions of the new resonance involving the Higgs boson or longitudinally polarized SM vector bosons;

c_f describes the direct interactions of the new resonance with fermions;

g_V is the typical strength of the new interaction;

M_V is the mass of the new resonance.

The W' and Z' bosons couple to the fermions through the combination of parameters $g^2 c_f / g_V$ and to the Higgs and vector bosons through $g_V c_H$, where g is the $SU(2)_L$ gauge coupling.

The production of W' and Z' at hadron colliders is dominated by the process $q\bar{q}^{(\prime)}/q\bar{q} \to W'/Z'$. Two benchmark models are provided in Ref. [19]. In model A, weakly coupled vector resonances arise from an extension of the SM gauge group such as the SSM. In model B, the heavy vector triplet is produced in a strongly coupled scenario, for example in a Composite Higgs model. Consequently, in model A, the branching fractions to fermions and gauge bosons are comparable, whereas for model B, fermionic couplings are suppressed. Therefore, in the context of WW, WZ, ZH, and WH resonance searches, the scenario of model B is of higher interest, since the scenario of model A have been strongly constrained by searches in final states with fermions. Since model B is inspired by a strongly coupled scenarios of electroweak symmetry breaking, i.e. Composite Higgs models, it has to be considered in the region $g_V \gtrsim 3$. A value of $g_V = 3$ is usually chosen, which assures a reasonably small natural width with respect to the experimental resolution. Hence, we consider the model B scenario with parameters $g_V = 3$, $c_H = -1$ and $c_f = 1$, where the heavy resonances couples to W' and Z' as a SM custodial triplet, i.e. where we expect W' and Z' to be degenerate in mass and the branching fractions $\mathcal{B}(W' \to WH)$ and $\mathcal{B}(Z' \to ZH)$ are comparable to $\mathcal{B}(W' \to WZ)$ and $\mathcal{B}(Z' \to WW)$. In addition, we consider also heavy resonances that couple to W' and Z' as a SM singlet, i.e. only a charged or a neutral resonance is expected at a given mass.

For a W' with SM couplings to fermions (model A, $g_V = 1$) and thus reduced decay branching ratio to SM bosons, the most stringent limits on production cross sections obtained with 8 TeV collision data are reported in searches with leptonic final states [23, 24]. The lower mass limit

obtained on the W′ mass is 3.3 TeV. This mass limit has been superseded by the more stringent limit of 4.4 TeV obtained in the corresponding 13 TeV search [25]. In the same context, searches for a W′ decaying into a pair of SM vector bosons (WZ,WH) with 8 TeV data provide a lower mass limit of 1.81 TeV (in model A, $g_V = 1$) [10, 12, 13, 26–28]. This limit has been increased by the corresponding 13 TeV search to a value of 2.1 TeV (in model B) [7].

For a Z′ with SM couplings to fermions (model A, $g_V = 1$) and thus reduced decay branching ratio to SM bosons, the most stringent limits on production cross sections obtained with 8 TeV collision data are reported in searches with two leptons in the final states [29, 30]. These results exclude a Z′ with a mass lower than 2.90 TeV. This mass limit has been superseded by the more stringent limit of 3.15 TeV obtained in the corresponding 13 TeV search [31]. In the same context, searches for a Z′ decaying into a pair of SM vector bosons (WW,ZH) with 8 TeV data provide a lower mass limit of 1.4 TeV (in model A, $g_V = 1$) [11, 14, 32].

The most stringent limit on a heavy vector triplet resonance was set at 1.8 TeV (in model B) obtained from a combination of 8 TeV VH searches [11, 13].

2.2 Spin-2 resonances

Massive resonances of spin-2 can be generically motivated in warped extra dimensional models [1, 2] that predict the existence of a so-called tower of Kaluza–Klein (KK) excitations of a spin-2 boson, the KK graviton. The original RS model (here denoted as RS1) can be extended to the bulk scenario (G_{bulk}), which addresses in addition the flavor structure of the SM through localization of fermions in the warped extra dimension [16–18].

These models have two free parameters: the mass of the first mode of the KK bulk graviton, M_G, and the ratio $\tilde{k} \equiv k/\overline{M}_{Pl}$, where k is the unknown curvature scale of the extra dimension, and $\overline{M}_{Pl} \equiv M_{Pl}/\sqrt{8\pi}$ is the reduced Planck mass. The constant $\tilde{k}$ acts as the coupling constant of the model, on which the production cross-sections and widths of the graviton depend quadratically. For models with $\tilde{k} \lesssim 0.5$, the natural width of the resonance is sufficiently small to be neglected when compared to the detector resolution.

In the bulk scenario, coupling of the graviton to light fermions is highly suppressed and the decay into photons is negligible, while in the RS1 scenario branching ratios to photons and fermions are dominant. The production of gravitons at hadron colliders in the bulk scenario is thus dominated by gluon-gluon fusion, while in the RS1 scenario $q\bar{q}$ and gluon-gluon fusion production contribute equally. The resulting production cross section in the bulk scenario is of order 10^4 times lower than in the RS1 scenario. However, in the context of WW and ZZ resonance searches, the bulk scenario is of higher interest, since the RS1 scenario has been strongly constrained in searches with final states with fermions and photons. The two models also differ in the polarization of the produced W and Z bosons. The RS1 graviton decays to transverse polarized bosons 90% of the time, while the bulk graviton decays to longitudinal polarized bosons more than 99% of the time. This leads to differences in the efficiency of the techniques used for identifying the bosons.

In the scenario with $\tilde{k} = 1$, where the bulk graviton has comparable or larger width than the detector resolution, the most stringent limit of 0.81 TeV on the bulk graviton mass was set by a combination of searches in the diboson final state [15, 26, 27]. The most stringent limits on the cross section for narrow bulk graviton resonances in the scenario of $\tilde{k} \lesssim 0.5$ were set by searches in the diboson final state [7, 9, 10]; however, no limits on the resonance mass could be set due to the low predicted production cross section.

Table 1: Summary of the properties of heavy resonances considered in the combination.

particle	spin	charge	decay	production	W/Z polarization
W′	1	charged	mainly WZ, WH	mainly $q\bar{q}^{(\prime)}$	mostly longitudinal
Z′	1	neutral	mainly WW, ZH	mainly $q\bar{q}$	mostly longitudinal
G_{bulk}	2	neutral	mainly WW, ZZ	mainly gg	mostly longitudinal

3 Data analyses

3.1 8 TeV VV searches

Searches for new heavy resonances decaying into a pair of vector bosons (WW, ZZ or WZ) have been performed by the CMS Collaboration with the proton-proton collision data collected at $\sqrt{s}$ = 8 TeV and corresponding to an integrated luminosity of 19.7 fb^{-1}. The published results in the all-leptonic ($3\ell\nu$), semi-leptonic ($\ell\nu q\bar{q}$ and $\ell\ell q\bar{q}$), and all-hadronic ($q\bar{q}q\bar{q}$ or dijet) final states are included in the statistical combination described in this note and summarized in the following.

3.1.1 8 TeV $3\ell\nu$ analysis

The $3\ell\nu$ analysis channel searching for WZ resonances is described in detail in Ref. [12]. The Z boson candidate is reconstructed requiring two opposite-sign, same-flavor lepton pairs (muons or electrons) with invariant mass between 71 and 111 GeV. This requirement makes the contribution from $Z \to \tau\tau \to \ell\nu\nu\ell\nu\nu$ events negligible compared to the other dilepton decays; because of the escaping neutrinos the dilepton invariant mass is much smaller than the nominal Z boson mass. Events with two distinct Z boson candidates, where the candidates do not share a lepton, are rejected in order to suppress the ZZ background. With this requirement and considering the low dilepton decay branching fraction, the contamination from signals decaying to a pair of Z bosons in the all-leptonic final state is negligible.

A candidate for the charged lepton from the decay of a W boson is then selected out of the remaining leptons. When several candidates are found, the one with the highest p_T is selected. The missing transverse energy E_T^{miss} is defined as the magnitude of the projection on the plane perpendicular to the beams of the negative vector sum of the momenta of all the reconstructed particles in the event, and it is required to be larger than 30 GeV. The identified lepton and the E_T^{miss} are then combined to reconstruct the $W \to \ell\nu$ candidate. In order to fully reconstruct the WZ candidate, the longitudinal component of the neutrino momentum is calculated by solving a second-order equation that sets the $\ell\nu$ invariant mass to be equal to the known W boson mass.

The results are interpreted in the context of a W′ resonance decaying to WZ. Exclusion limits at 95% CL on the production cross section $\sigma(pp \to W' \to WZ) \times BR(WZ \to 3\ell\nu)$ are determined for each signal mass hypothesis using a counting experiment, which compares the number of observed events to the number of expected signal and background events.

3.1.2 8 TeV $\ell\nu q\bar{q}$ and $\ell\ell q\bar{q}$ analyses

The $\ell\nu q\bar{q}$ and $\ell\ell q\bar{q}$ analysis channels are described in detail in Ref. [9]. These searches are limited to final states where $\ell = \mu$ or e; however the results include the case in which $W \to \tau\nu$ or $Z \to \tau\tau$ where the tau decay is $\tau \to \ell\nu\nu$. The $\ell\nu q\bar{q}$ channel requires exactly one isolated lepton with $p_T > 50$ GeV or $p_T > 90$ GeV if reconstructed as a muon or an electron, respectively. The value of E_T^{miss} is required to be larger than 40 (80) GeV for the muon (electron) channel. The identified electron or muon and E_T^{miss} are combined to reconstruct the $W \to \ell\nu$ candidate following a procedure similar to that described for the $3\ell\nu$ analysis channel. The $W \to \ell\nu$

candidate is required to have $p_T > 200$ GeV. In the $\ell\ell q\bar{q}$ channel, exactly two leptons with the same flavor (muons or electrons) and opposite charge are required. In the case in which two muons are reconstructed an asymmetric threshold of 40 and 20 GeV is applied to their p_T, while in the case of two electrons a threshold of 40 GeV is required for both. The invariant mass of the dilepton system is required to be between 70 and 110 GeV. Finally, the Z boson candidate is required to have $p_T > 80$ GeV.

In both analysis channels, jets used for identifying the hadronically decaying W and Z bosons are clustered using the Cambridge–Aachen (CA) algorithm [33] with distance parameter $R = 0.8$ ("CA8 jets"). Hadronic V-boson candidates, also referred as V jets, are selected with $p_T > 200$ (80) GeV in the single-lepton (dilepton) channel and $|\eta| < 2.4$. In the semi-leptonic channel, jets are also identified using the anti-k_T jet-clustering algorithm [34] with distance parameter $R = 0.5$ ("AK5 jets"). In order to further reduce the level of the $t\bar{t}$ background, events are rejected if one or more AK5 jets is identified as originating from the hadronization of a b quark (b-tagged jet). Since the AK5 jets might overlap with the V jet candidate, this analysis channel is not sensitive to the case in which the Z boson from $W' \to WZ$ decays into the $b\bar{b}$ final state. Furthermore, this requirement makes the contamination from $W' \to WH \to \ell\nu b\bar{b}$ signal negligible.

In order to discriminate against quark and gluon jet background, selections on the jet substructure quantities pruned jet mass [35, 36] and N-subjettiness τ_{21} [37] are applied to the CA8 jet. The V jet candidate is identified in the $\ell\nu q\bar{q}$ channel if its pruned mass, m_{jet}, falls in the range $65 < m_{jet} < 105$ GeV. Similarly, a V jet candidate in the $\ell\ell q\bar{q}$ channel is required to have $70 < m_{jet} < 110$ GeV. To enhance the analysis sensitivity, two V jet categories are distinguished:

- high-purity (HP) category: $\tau_{21} < 0.5$;
- low-purity (LP) category: $0.5 < \tau_{21} < 0.75$.

The total efficiency of the m_{jet} and τ_{21} HP selection criteria for a signal of mass 2 TeV is about 45% with a mistagging rate of 2% [10]. Although it is expected that the HP category dominates the total sensitivity of the analysis, the LP category has been retained, since for large masses of a new resonance it provides improved signal efficiency with only moderate background contamination. The final categorization is based on four classes of events, depending on their lepton flavor (muon or electron) and V jet purity (LP and HP). The selection efficiencies for each signal are summarized separately for the HP and LP categories in Table 2.

The dominant background in the two channels originates from the SM production of V+jets events; less important contributions are given by pair-produced top quarks and non-resonant diboson processes. The shape of the invariant mass distribution and the normalization for the V+jets dominant background are determined from data in a signal-depleted control region around the m_{jet} window that defines the signal region. For the $\ell\nu q\bar{q}$ channel, lower and upper sideband regions are defined in the m_{jet} ranges (40, 65) and (105, 130) GeV, respectively. In the $\ell\ell q\bar{q}$ channel, the sidebands are defined in the m_{jet} ranges (50, 70) and (110, 130) GeV. Only the lower sideband is used to estimate the background shape, while the overall background normalization is estimated considering the observed data distribution in the high sideband as well, which potentially contains signal from a $WH \to \ell\nu b\bar{b}$ resonance. However, this contamination is found to have negligible impact on the resulting background estimate considering the W' signal cross section excluded by these analyses. Shape and normalization of minor backgrounds are estimated from simulation. The dominant backgrounds and their estimation methods are summarized in Table 3.

Exclusion limits at 95% CL have been set on the production cross section of a bulk graviton.

Table 2: Summary of the signal efficiencies of all analysis channels for all signal models for a 2 TeV resonance in both high-purity (HP) and low-purity (LP) categories. The signal efficiencies are in percent and include the branching ratios of the two vector bosons to the final state of the analysis channel, effects from detector acceptance, as well as reconstruction and selection efficiencies.

Channel	HVT				RS bulk	
	W'		Z'		G_{bulk}	
	WZ	WH	WW	ZH	WW	ZZ
	HP/LP	HP/LP	HP/LP	HP/LP	HP/LP	HP/LP
$q\bar{q}q\bar{q}$ (8 TeV)	5.9/5.5	0.8/0.7	5.7/5.3	0.8/0.7	3.8/3.1	5.7/4.2
$\ell\nu q\bar{q}$ (8 TeV)	4.8/-	-	9.4/-	-	10.6/7.1	-
$\ell\ell q\bar{q}$ (8 TeV)	1.1/-	-	-	0.2/-	-	3.0/1.0
$3\ell\nu$ (8 TeV)	0.6	-	-	-	-	-
$q\bar{q}q\bar{q}$ (13 TeV)	5.0/10.1	1.8/2.5	4.2/8.7	1.9/2.6	4.5/10.2	5.7/11.2
$\ell\nu q\bar{q}$ (13 TeV)	9.4/0.5	1.7/0.2	19.0/1.1	-	16.7/1.0	-
$q\bar{q}b\bar{b}/q\bar{q}q\bar{q}q\bar{q}$ (8 TeV)	-	3.0/1.8	-	1.7/1.1	-	-
$\ell\nu b\bar{b}$(8 TeV)	-	0.9	-	-	-	-
$q\bar{q}\tau\tau$ (8 TeV)	-	1.2	-	1.3	-	-
$\ell\ell b\bar{b}$ (13 TeV)	-	-	-	1.5	-	-
$\ell\nu b\bar{b}$ (13 TeV)	-	4.0	-	-	-	-
$\nu\nu b\bar{b}$ (13 TeV)	-	-	-	4.2	-	-

The results were published with a parametrization for the reconstruction efficiency as a function of W and Z boson kinematics, enabling a reinterpretation in the context of the HVT model B described in Section 2.1, which predicts the production of charged and neutral spin-1 resonances decaying preferably to WW and WZ. The reinterpretation in the context of this model is obtained by rescaling the bulk graviton signal efficiencies by scale factors taking into account the different kinematics of W and the Z bosons from W′ and Z′ production compared to the graviton production. The scale factors have been derived for each mass point by means of the tables published in Ref. [9]. Since the efficiency parametrization is restricted to the HP category of the analyses, the LP category is not used for the HVT W′ and Z′ interpretations of these channels. The m_{jet} window that defines the signal regions of the analysis channels is such that the $\ell\nu q\bar{q}$ channel is sensitive to both the charged and neutral resonance predicted by HVT models. This is taken into account in the combination presented in Section 5.3.

3.1.3 8 TeV $q\bar{q}q\bar{q}$ analysis

The analysis channel in which each of the two bosons decay hadronically is described in detail in Ref. [10]. As for the semi-leptonic case, the two V jet candidates are reconstructed by means of the CA jet algorithm with distance parameter R=0.8. Events are selected by requiring at least two jets with $p_T > 200$ GeV and $|\eta| < 2.5$. The two jets of highest p_T are required to have a separation $|\Delta\eta| < 1.3$ to reduce background from multijet events. The invariant mass of the two selected jets is required to have $m_{jj} > 890$ GeV, which leads to 99% trigger efficiency, with a negligible systematic uncertainty. The CA8 jets are required to pass certain noise rejection requirements that effectively reject well identified muons and electrons clustered into a jet. Less than 1% of the events decaying to WW or ZZ that pass the event selection criteria are from $WW \to \ell\nu q\bar{q}$ or $ZZ \to \ell\ell q\bar{q}$ decays, where ℓ refers to a muon or an electron. Further, less than 1% of the selected WW events are from $WW \to \tau\nu q\bar{q}$ decays, and only 3% of the selected ZZ events correspond to $ZZ \to \tau\tau q\bar{q}$ decays.

Table 3: Summary of the dominant backgrounds and their estimation methods in each analysis channel.

Channel	Main background	Estimation method
$q\bar{q}q\bar{q}$ (8 TeV)	QCD multijets	parametrized by smooth function
$\ell\nu q\bar{q}$ (8 TeV)	W+jets	normalization and shape from data in sidebands: m_{jet} in [40, 65] and [105, 130] GeV
$\ell\ell q\bar{q}$ (8 TeV)	Z+jets	normalization and shape from data in sidebands: m_{jet} in [50, 70] and [110, 130] GeV
$q\bar{q}q\bar{q}$ (13 TeV)	QCD multijets	parametrized by smooth function
$\ell\nu q\bar{q}$ (13 TeV)	W+jets	normalization and shape from data in sidebands: m_{jet} in [40, 65] and [135, 150] GeV
$q\bar{q}b\bar{b}/q\bar{q}q\bar{q}q\bar{q}$ (8 TeV)	QCD multijets	data driven
$\ell\nu b\bar{b}$ (8 TeV)	W+jets	normalization and shape from sidebands: m_{jet} in [40, 110] and [135, 150] GeV
$q\bar{q}\tau\tau$ (8 TeV)	Z/γ+jets $t\bar{t}$, QCD multijets	data driven estimate from control regions
$\ell\ell b\bar{b}/\ell\nu b\bar{b}/$ $\nu\nu b\bar{b}$ (13 TeV)	V+jets	normalization and shape from data in sidebands: m_{jet} in [30, 65] and $>$ 135 GeV

Similar to the semi-leptonic case, jet pruning and N-subjettiness algorithms are applied to the V jet candidates. If the pruned jet has a mass within $70 < m_{jet} < 100$ GeV, it is tagged as a V jet candidate. Both selected jets are required to be V-tagged. In addition, at least one of the two V jets is required to pass the τ_{21} HP selections defined as for the semi-leptonic case. Finally, the analysis is divided in HP and LP categories, depending on whether the other V-tagged jet is in the high purity or low purity τ_{21} region. The selection efficiencies for each signal and category are summarized in Table 2.

The dominant background consists of multijet events from QCD processes. The dijet background is estimated using a fit of a smoothly falling parametric function to the mass spectrum observed in data. Only diboson resonances with M_V or $M_G > 1$ TeV are considered in this analysis channel. The dominant backgrounds and their estimation methods are summarized in Table 3.

The results have been combined with the $\ell\nu q\bar{q}$ and $\ell\ell q\bar{q}$ analysis channels and interpreted in the context of the bulk graviton model in the narrow-width approximation. The dijet analysis results have also been interpreted in Ref. [10] in the context of a W' resonance; hence a Z' reinterpretation was added. The m_{jet} window that defines the signal regions of the analysis is such that the dijet channel is sensitive to both the charged and neutral resonance predicted by HVT models. This is taken into account in the combination presented in Section 5.3.

3.2 13 TeV VV searches

3.2.1 13 TeV $\ell\nu q\bar{q}$ and $q\bar{q}q\bar{q}$ analyses

The VV searches performed with 8 TeV data and described in the previous section have been repeated with the proton-proton collision data collected at $\sqrt{s}$ = 13 TeV. The results in the $\ell\nu q\bar{q}$ and $q\bar{q}q\bar{q}$ channels, corresponding to an integrated luminosity of 2.2–2.6 fb^{-1}, are reported in Ref. [7]. The same strategies as for the 8 TeV analyses have been followed and only the main differences are highlighted below.

In both channels the hadronically decaying vector bosons are reconstructed by means of the anti-k_T algorithm with distance parameter $R = 0.8$. Both jet pruning and N-subjettiness algorithms are exploited to discriminate against quark and gluon jet background. Differently from the 8 TeV case, the m_{jet} requirement has been optimized simultaneously for the two analyses and for both W jet and Z jet signals. The optimization resulted in a common signal region defined in the range (65,105) GeV. The categorization follows a slightly different scheme with respect to the 8 TeV analyses: in addition to τ_{21} categories, pruned jet mass categories have been added to enhance the analysis sensitivity to different signal hypotheses. The mutually exclusive m_{jet} categories are:

- W jets enriched category: $65 < m_{jet} < 85$ GeV; dominantly sensitive to resonances decaying into W bosons (e.g. $G_{bulk}/Z' \to WW$ in the $\ell\nu q\bar{q}$ channel)
- Z jets enriched category: $85 < m_{jet} < 105$ GeV; dominantly sensitive to resonances decaying into Z bosons (e.g. $G_{bulk} \to ZZ$, $W' \to WZ$ in the $\ell\nu q\bar{q}$ channel)

As for the 8 TeV case, HP and LP τ_{21} categories have been defined even though two different working points are used for the two channels as a result of an optimization. For the semi-leptonic channel, HP and LP V jets are selected by requiring $\tau_{21} < 0.6$ and $0.6 < \tau_{21} < 0.75$, respectively. For the all-hadronic channel, where the background rate is much higher, a tighter working point of 0.45 is preferred. The total efficiency and the mistagging rate of the m_{jet} and HP selection criteria for the τ_{21} working point of 0.45 for a signal with a mass of 2 TeV are 35% and 1.8%, respectively. The final number of categories is eight and six in the semi-leptonic (including electron and muon) and all-hadronic channels, respectively. The selection efficiencies for each signal and category are summarized in Table 2.

As in the 8 TeV case, in the semi-leptonic channel jets are also identified using the anti-k_T jet-clustering algorithm with distance parameter $R = 0.4$ ("AK4 jets"). Differently from the 8 TeV case, AK4 jets are required to be separated from the V jet candidate by $\Delta R = \sqrt{(\Delta\eta)^2 + (\Delta\phi)^2} > 0.8$. In order to further reduce the level of the $t\bar{t}$ background, events are rejected if one or more AK4 jets is b-tagged. Since in this case the AK4 jets cannot overlap with the V jet candidate, this analysis channel is sensitive to the case in which the Z boson from a $W' \to WZ$ signal decays into the $b\bar{b}$ final state.

In the $\ell\nu q\bar{q}$ channel the W+jets dominant background is estimated from a control region around the m_{jet} windows. Lower and upper sideband regions are defined in the m_{jet} ranges (40, 65) and (135, 150) GeV, respectively. The Higgs boson mass region, defined in the range (105, 135) GeV, has been kept blinded in order to avoid overlap with analysis channels with hadronically decaying Higgs bosons in the final state. In order to accomplish this the high sideband has been moved to higher values compared to the 8 TeV case, where, on the contrary, it overlaps with the Higgs boson mass window. The dominant backgrounds and their estimation methods are summarized in Table 3.

The results of the two analyses have been combined in the context of bulk graviton model and

W′ of HVT model B.

3.3 8 TeV VH searches

Searches for new heavy resonances decaying into a vector boson (W or Z) and a Higgs boson have been performed in within the CMS Collaboration with the proton-proton collision data collected at $\sqrt{s}$ = 8 TeV and corresponding to an integrated luminosity of 19.7 fb^{-1}. The searches cover both semi-leptonic and all-hadronic final states with the Higgs boson decaying into a pair of bottom quarks, tau leptons or W bosons. The searches in the individual channels [11, 13, 14] are summarized in the following.

3.3.1 8 TeV $\ell\nu b\bar{b}$ analysis

The search for a resonance W′ decaying into a W and a Higgs boson in the $\ell\nu b\bar{b}$ final state is described in detail in Ref. [13]. This search is limited to final states where $\ell = \mu$ or e; however the results include the case in which $W \to \tau\nu$. The search strategy is closely related to the search for WV resonances in the $\ell\nu q\bar{q}$ final state described above, and only the main differences are mentioned below. As for the analyses involving boosted vector bosons, CA8 jets are used to identify Higgs-initiated jets (H jets). Discrimination against quark and gluon jet background is again obtained by means of the jet pruning algorithm: a jet is considered as an H-tagged jet if its pruned mass falls in the range $110 < m_{\text{jet}} < 135$ GeV. Additional discrimination against the background is gained exploiting b tagging methods that discriminate jets originating from b quarks against those originating from lighter quarks or gluons ("H_{bb} tagging"). The b tagging algorithm is applied to the two individual subjets in which the H jet candidate is split, depending on their angular distance: if the two subjets are close to each other (ΔR <0.3), inefficiencies of the algorithm are recovered by applying b tagging to the whole jet. To further reduce the level of the $t\bar{t}$ background, events are rejected if one or more b-jets, not overlapping with the H jet candidate, are identified, and if the reconstructed mass of the hadronically or leptonically decaying top quark candidate lies in a window around the nominal top quark mass.

The dominant backgrounds originate from the SM production of W+jets events, followed by pair-produced top quarks and by non-resonant diboson processes. The background estimation follows the same data-driven procedure described for the VV case. Lower and upper sideband regions are defined in the m_{jet} ranges (40, 110) and (135, 150) GeV, respectively. The dominant backgrounds and their estimation methods are summarized in Table 3. The observed data in the muon channel are found compatible with the predicted background in the signal region, while in the electron channel, an excess of three events is observed at $M_{WH} \approx 1.8$ TeV. The local significance of the excess is 2.9 standard deviations, which translates into a global significance of 1.9 standard deviations, searching for resonances over the full mass range 0.8–2.5 TeV and across two channels.. Exclusion limits are set in the context of the HVT model B W′.

3.3.2 8 TeV $q\bar{q}\tau\tau$ analysis

The second analysis channel with the Higgs boson in the final state considered for the combination is the search for a resonance Z′ decaying into Z and Higgs bosons in the $q\bar{q}\tau\tau$ final state [11]. This search includes six channels corresponding to all the combinations of tau lepton decays: three all-leptonic, two semi-leptonic, and one all-hadronic. As in the other searches described above in this section, CA8 jets are used to identify the hadronically decaying Z boson. Events are selected by requiring a Z jet candidate with $p_{\text{T}} > 400$ GeV, pruned jet mass m_{jet} in the range $70 < m_{\text{jet}} < 110$ GeV, and $\tau_{21} < 0.75$.

While the Z jet selection is common to all the channels considered, the reconstruction of the $\tau\tau$

system is performed differently depending on the τ decay channel and dedicated techniques for the high energy ranges given by these searches are exploited. Electrons and muons are selected if $p_T > 10$ GeV. Hadronically decaying tau leptons (τ_h) are identified starting from jets clustered using the anti-k_T algorithm with distance parameter $R = 0.5$ and selected if they have $p_T > 20$ GeV. Because the unobserved neutrinos from tau lepton decays can carry a significant fraction of the $\tau\tau$ energy and momenta, the E_T^{miss} is required to be larger than 100, 50, and 80 GeV in the all-leptonic, semi-leptonic, and all-hadronic channel, respectively. The visible momenta in the $\tau\tau$ decay are combined with E_T^{miss} to reconstruct the kinematics of the parent boson. For the $\tau\tau$ system, $p_T > 100$ GeV is required. Furthermore, $m_{\tau\tau}$ is required to be in the range (105, 180) GeV in the all-hadronic channel. An upper limit of 1.0 is placed on $\Delta R_{\ell\ell}$ in order to reject the W+jets background. Finally, events with identified b jets, not overlapping with the τ candidates, are discarded in order to reduce the level of the $t\bar{t}$ background in the all-leptonic and semi-leptonic channels.

Because of the non-uniformity of the background composition across the analysis channels, different estimation techniques based on data are used in each. For the all-leptonic channel, shape and normalization of the dominant Z/γ+jets background are estimated from data in a control region around the m_{jet} window that defines the signal region including only events with $\tau_{21} > 0.75$. The lower and upper sideband regions are defined in the m_{jet} ranges (20, 70) and (140, 200) GeV, respectively. For the semi-leptonic channel, shape and normalization of the dominant $t\bar{t}$ background is estimated from data in a control region defined as the signal region but requiring at least one b-tagged jet. Finally, in the all-hadronic channel the total background normalization in the signal region is estimated from the relative amount of data in three control regions defined in the (m_{jet},$m_{\tau\tau}$) plane.

The results have been interpreted in the context of the HVT model B predicting a neutral spin-1 Z' resonance decaying into Z and Higgs bosons [11]. Given the large m_{jet} window used to tag the hadronically decaying Z boson, this analysis channel is also sensitive to the production of the charged spin-1 W' resonance decaying into W and Higgs bosons as predicted in HVT models. This overlap is taken into account in the statistical combination described in Section 5.3.

3.3.3 8 TeV $q\bar{q}b\bar{b}$/$q\bar{q}q\bar{q}q\bar{q}$ analysis

Finally, the search for a charged (W') or neutral (Z') resonance decaying into a Higgs boson and a W or Z boson in the all-hadronic final state [14] is considered. The final states with $H \to b\bar{b}$ and $H \to WW^* \to 4q$ are included in this search. As in the analogous VV dijet analysis, the V jet and H jet candidates are reconstructed by means of the CA jet algorithm with distance parameter $R = 0.8$. The two jets of highest p_T are required to have separation $|\Delta\eta| < 1.3$ to reduce background from multijet events. The invariant mass of the two selected jets is required to have $m_{jj} > 890$ GeV in order to follow the trigger acceptance. Jet pruning and N-subjettiness algorithms are applied to the V jet and H jet candidates. If the pruned jet has mass m_{jet} within $70 < m_{jet} < 100$ GeV ($110 < m_{jet} < 135$ GeV), it is tagged as a W/Z (H) candidate. In order to tag jets from $H \to b\bar{b}$ decays, the same b tagging procedure as in the semi-leptonic $\ell\nu b\bar{b}$ search is applied. Finally, high and low-purity V jets are selected by requiring $\tau_{21} < 0.5$ and $0.5 < \tau_{21} < 0.75$, respectively; high and low-purity H_{WW}-jets are selected by requiring the N-subjettiness quantity $\tau_{42} < 0.55$ and $0.55 < \tau_{42} < 0.65$.

The dominant background consists of multijet events from QCD processes. The dijet background is estimated using a fit of a smoothly falling parametric function to the mass spectrum observed in data. The dominant backgrounds and their estimation methods are summarized in Table 3.

The results are interpreted in the context of the HVT model B predicting both charged and neutral spin-1 resonances decaying into a Higgs boson and a W or Z boson.

The three VH channels described in this section have also been combined in the context of the HVT model B, improving the lower limit up to 1.8 TeV [13]. The selection efficiencies for each signal and category are summarized in Table 2.

3.4 13 TeV VH searches

3.4.1 13 TeV $\ell\ell b\bar{b}/\ell\nu b\bar{b}/\nu\nu b\bar{b}$ analyses

Searches for new heavy resonances decaying into a vector boson (W or Z) and a Higgs boson have been performed using 2.17–2.52 fb^{-1} of data collected at $\sqrt{s}$ = 13 TeV. The results, reported in Ref. [8], considered the leptonic vector boson decays (Z$\to \nu\nu$, W$\to \ell\nu$, and Z$\to \ell\ell$, with ℓ = e, μ), while the Higgs boson decays into a $b\bar{b}$ pair. As in the analyses involving boosted vector bosons performed with 13 TeV collision data, AK8 jets are used to identify H jets. The analysis strategy follows the analogous VH analyses performed with 8 TeV collisions data: the pruning and the subjet b tagging algorithms are used to discriminate against quark and gluon jet background.

Events are divided into categories depending on the number (0, 1 or 2) and flavor (e or μ) of the reconstructed charged leptons, and the presence of 1 or 2 b-tagged subjets. In total, 10 exclusive categories are defined. In the zero-lepton category candidate signal events are expected to have large $E_{\mathrm{T}}^{\mathrm{miss}}$ due to the boosted Z boson decaying into a pair of neutrinos, which escape undetected. Hence, a tight selection is applied on the reconstructed $E_{\mathrm{T}}^{\mathrm{miss}}$, which is required to be larger than 200 GeV. A veto is applied to isolated leptons with $p_{\mathrm{T}} > 10$ GeV, hadronically-decaying τ leptons and photons in order to reduce the contribution of SM processes. The $t\bar{t}$ background contribution is reduced by rejecting events with one or more b-jets, not overlapping with the H jet candidate. Due to the lack of visible decay products from the Z boson, a reconstruction of the resonance mass is not directly viable. Instead, the H jet momentum and the $E_{\mathrm{T}}^{\mathrm{miss}}$ are used to compute the transverse mass $m_{\mathrm{T}} = \sqrt{2E_{\mathrm{T}}^{\mathrm{miss}}E_T^{jet}(1-\cos\Delta\phi(jet, E_{\mathrm{T}}^{\mathrm{miss}}))}$. Events in the single-lepton channel are selected requiring exactly one reconstructed muon or electron with p_{T} larger than 55 GeV and 135 GeV, respectively, passing tight identification and isolation requirements. Events with other leptons passing looser selections or hadronic τ leptons are discarded. In the single electron channel, multijet background is reduced by requiring $E_{\mathrm{T}}^{\mathrm{miss}} > 80$ GeV. As for the zero-lepton selection, the veto on additional b-tagged jets is applied. The four-momentum of the W candidate is quantified using a method similar to that used in the semi-leptonic VV and VH analyses. The W candidate is also required to have $p_{\mathrm{T}} > 200$ GeV. In the di-lepton channel an additional isolated muon or electron, with the same flavor and opposite charge of the leading one, is required to be reconstructed and identified. The Z boson candidates are considered only if the di-lepton invariant mass lies between 70 GeV and 110 GeV with $p_{\mathrm{T}} > 200$ GeV.

The Higgs boson candidate is reconstructed with the same criteria in all the considered categories, selecting the highest-p_{T} AK8 jet in events with at least one jet with $p_{\mathrm{T}} > 200$ GeV and a pruned mass $105 < m_{\mathrm{jet}} < 135$ GeV. In order to discriminate against the large background given by vector boson production in association with light-flavored jets, events are classified according to the number of subjets (1 or 2) passing the b tagging selection. The 2 b tags category offers a higher discrimination against the background, and dominates the sensitivity in the lower mass spectrum. However, the subjet b tagging algorithm is inefficient at high resonance masses due to the proximity of the two subjets. The 1 b tag category allows us to

recover the efficiency lost at high mass, but it is not competitive at low mass due to the large background contamination. This approach results in performance similar to the fat-jet/subjet b tagging algorithm used in the 8 TeV VH analyses. The selection efficiencies for each signal are summarized in Table 2.

The main source of background events originates from the production of a vector boson in association with jets and the subsequent decay of the vector boson into one of the considered leptonic final states. A sizeable background originates from b jets and W bosons from top quark decays. Minor contributions come from single top quark, diboson (VV and VH), and multijet productions. The background estimation follows the same data driven procedure described for the semi-leptonic VV and WH case. Lower and upper sideband regions are defined in the m_{jet} ranges (30, 65) and $m_{\text{jet}} > 135$ GeV, respectively. The dominant backgrounds and their estimation methods are summarized in Table 3.

The results have been interpreted in the context of the HVT model B under the singlet hypotheses of a spin-1 charged W′ or a neutral Z′ resonance decaying into W or a Z boson and a Higgs boson, respectively [8].

4 Combination procedure

For each analysis and signal hypothesis a likelihood function is constructed from the reconstructed diboson invariant mass distribution observed in data, the background prediction, and the signal resonance shape to test for the presence of a new resonance decaying to two bosons. For the $3\ell\nu$, $\mathrm{q\bar{q}q\bar{q}}$, $\mathrm{q\bar{q}b\bar{b}}$/$\mathrm{q\bar{q}q\bar{q}q\bar{q}}$, and $\mathrm{q\bar{q}}\tau\tau$ analyses, the likelihood function $\mathcal{L}$, computed using events binned as a function of reconstructed diboson invariant mass, is

$$\mathcal{L}(\mu; \text{data}) = \prod_i \frac{\lambda_i^{n_i} \mathrm{e}^{-\lambda_i}}{n_i!}, \tag{1}$$

where $\lambda_i = \mu N_i(S) + N_i(B)$, μ is a scale factor for the signal, $N_i(S)$ is the number expected from the signal in the i^{th} mass bin, and $N_i(B)$ is the number expected from background. The parameter n_i is the number of data events in the i^{th} mass bin. For the remaining analyses ($\ell\nu\mathrm{q\bar{q}}$, $\ell\ell\mathrm{q\bar{q}}$, $\ell\nu\mathrm{b\bar{b}}$), the likelihood is similarly defined using functional forms that describe the shape of the reconstructed diboson invariant mass for background and signal resonance, and a scale factor μ for the signal.

We search for a peak on top of the falling background spectrum by means of a maximum likelihood fit to the data. The likelihood is maximized to obtain the best fit μ for each signal and resonance mass hypothesis. The treatment of the background in the maximum likelihood fit depends on the analyses channel. In the $\mathrm{q\bar{q}q\bar{q}}$ and $\mathrm{q\bar{q}b\bar{b}}$/$\mathrm{q\bar{q}q\bar{q}q\bar{q}}$ analyses, the background fit function parameters are left floating in the maximum likelihood fit, such that the background prediction is simultaneously obtained with the signal μ for every hypothesis. In the remaining analyses ($\ell\nu\mathrm{q\bar{q}}$, $\ell\ell\mathrm{q\bar{q}}$, $\ell\ell\mathrm{b\bar{b}}$, $\ell\nu\mathrm{b\bar{b}}$, $\nu\nu\mathrm{b\bar{b}}$), the background is estimated using data sidebands and uncertainties related to its parametrized shape are treated as nuisance parameters constrained with Gaussian probability density functions in the maximum likelihood fit. The analyses that are being combined have orthogonal event selections and do not select common data events. Cases of event overlap are explicitly stated in the Section 3.1 and have been found to be negligible. The likelihoods of the all channels are thus combined by constructing a combined likelihood from their product.

The dominant sources of systematic uncertainties are treated as nuisance parameters constrained with a log-normal probability density function. All nuisance parameters are profiled, i.e. for

each possible value of the parameter of interest μ they are refitted to maximize the likelihood function. When the likelihoods of multiple analyses channels are combined, the correlation of systematic effects across analysis channels is taken into account by categorizing the uncertainties into fully correlated (associate to same nuisance parameter) and fully uncorrelated (associate to different nuisance parameters). Table 4 summarizes which uncertainties are treated as correlated among 8+13 TeV analyses, e+μ channels, HP+LP categories and W+Z enriched categories in the combination.

Table 4: Correlation of systematic uncertainties.

Systematic uncertainty	Type	8+13 TeV	e+μ	HP+LP	W+Z
Lepton trigger	yield	no	no	yes	yes
Lepton identification	yield	no	no	yes	yes
Lepton momentum scale	yield, shape	no	no	yes	yes
Jet energy scale	yield, shape	no	yes	yes	yes
Jet energy resolution	yield, shape	no	yes	yes	yes
Jet mass scale	yield	no	yes	yes	yes
Jet mass resolution	yield	no	yes	yes	yes
b tagging	yield	no	yes	yes	yes
W tagging (HP/LP)	yield	no	yes	yes	yes
Integrated luminosity	yield	no	yes	yes	yes
Pileup	yield	no	yes	yes	yes
PDF	yield	yes	yes	yes	yes
μ_f,μ_r scales	yield	yes	yes	yes	yes

The most important and only nuisance parameters treated as correlated between 8 and 13 TeV analyses are those related to the parton distribution function (PDF) and the choice of factorization (μ_f) and renormalization (μ_r) scales used to estimate the signal cross sections. They have been re-evaluated for this combination for both 8 and 13 TeV analyses, estimating the full impact on the expected signal yield rather than the impact on only the signal acceptance. The PDF uncertainties are evaluated using the NNPDF 3.0 [38] PDFs. The uncertainty related to the choice of μ_f and μ_r scales is evaluated following the proposal in Refs. [39, 40] by varying the default choice of scales in the following 6 combinations of factors: $(\mu_f, \mu_r) \times (1/2, 1/2)$, $(1/2, 1)$, $(1, 1/2)$, $(2, 2)$, $(2, 1)$, and $(1, 2)$. The experimental uncertainties are all treated as uncorrelated between 8 and 13 TeV. At 13 TeV the systematic uncertainties are dominated by the statistical uncertainty of the datasets used to evaluate scale factors applied to the signal simulation to reproduce data.

The asymptotic approximation [41] of the CL_s criterion [42, 43] is used with the "LHC-style" test statistic [44] to set upper limits on the cross section for resonance production. When combining 8 and 13 TeV analyses, limits are set on the signal scale factor μ taking into account the production cross section ratio evaluated from theory between 8 TeV and 13 TeV.

5 Results

In this section the combination of the individual analysis channels described in Section 3 is presented, for each of the signal hypotheses summarized in Table 1. For each channel we present 95% CL exclusion limits on the signal production cross section times the relevant branching fractions, as well as on the ratio between the excluded cross section and the theoretical prediction, denoted $\sigma_{95\%}/\sigma_{\text{theory}}$ and referred to as the signal strength.

5.1 Limits on W′

Figure 1 (top left) shows the comparison and combination of the results obtained in the 8 TeV VV (Section 3.1) and VH (Section 3.3) searches. The 95% CL exclusion limits on the W′ production cross section times the branching fraction to WZ and WH in the resonance mass range $0.8 < m_{W'} < 2.9$ TeV are shown. Below resonance mass values of about 1.5 TeV, the $3\ell\nu$ channel is most sensitive. At higher masses the all-hadronic channel with the Higgs boson in the final state has approximately the same sensitivity as the $\ell\nu q\bar{q}$ and $q\bar{q}q\bar{q}$ channels. With the combination, the sensitivity on the cross section is improved by up to 50% over the whole mass range and a lower mass limit of 1.77 TeV is obtained.

Figure 1 (top right) shows the comparison and combination of the results obtained in the 13 TeV VV and VH searches. The combination includes the $\ell\nu q\bar{q}$ and $q\bar{q}q\bar{q}$ analysis channels described in Section 3.2 and the $\ell\nu b\bar{b}$ channel described in Section 3.4, and it covers the resonance mass range $0.8 < m_{W'} < 4$ TeV. The $\ell\nu q\bar{q}$ channel dominates the sensitivity at low masses ($\lesssim 1.8$ TeV), while at higher masses the all-hadronic channel is the most sensitive. W′ resonances with masses below 2.32 TeV are excluded by this statistical combination. This value supersedes the mass limit obtained from 8 TeV searches and it is slightly improved with respect to the value of 2.1 TeV obtained combining only the $\ell\nu q\bar{q}$ and $q\bar{q}q\bar{q}$ channels as reported in Ref. [7].

Figure 1 (bottom) shows the comparison and combination of the results obtained in the 8 and 13 TeV searches. The 95% CL exclusion limits on the signal strength in the resonance mass range $0.8 < m_{W'} < 4$ TeV are shown. Above resonance mass values of about 1.8 TeV, the 13 TeV searches dominate the sensitivity.

Figure 2 shows the comparison of the combination of 8 and 13 TeV results with the combination of only 8 TeV or only 13 TeV searches for the W′ signal hypothesis. The overall sensitivity benefits from the combination up to resonance masses of about 2 TeV, where the 8 TeV channels do not add any significant contribution. For resonance masses below 2 TeV, the sensitivity is improved by 20–70% with respect to the 13 TeV combination and by 10–40% compared to the 8 TeV combination. The observed mass limit is not affected by the combination compared to that obtained from the 13 TeV searches, which represents the most stringent to date in the context of diboson searches. However, the expected mass limit is slightly improved from 2.1 to 2.2 TeV.

5.2 Limits on Z′

Figure 3 (top left) shows the comparison and combination of the results obtained in the 8 TeV VV and VH searches. The 95% CL exclusion limits on the Z′ production cross section times the branching fraction to WW and ZH in the resonance mass range $0.8 < m_{W'} < 2.9$ TeV are shown. The $\ell\nu q\bar{q}$ channel dominates the sensitivity over the whole mass range. Nevertheless, with the combination the sensitivity on the cross section is improved by 20–30% depending on the resonance mass, with a significant contribution given by the $q\bar{q}q\bar{q}$ channel above 1 TeV. The lower mass limit of 1.69 TeV is comparable to the value reached by the $\ell\nu q\bar{q}$ channel only.

Figure 3 (top right) shows the comparison and combination of the results obtained in the 13 TeV VV and VH searches in the resonance mass range $0.8 < m_{Z'} < 4$ TeV. The combination includes the $\ell\nu q\bar{q}$ and $q\bar{q}q\bar{q}$ analysis channels described in Section 3.2 and the $\nu\nu b\bar{b}$ and $\ell\ell b\bar{b}$ channels described in Section 3.4. The semi-leptonic channels ($\ell\nu q\bar{q}$, $\ell\ell b\bar{b}$ and $\nu\nu b\bar{b}$) dominate the sensitivity at low masses ($\lesssim 2$ TeV), while at higher masses the sensitivity of the all-hadronic channel reaches that of the $\ell\nu q\bar{q}$ channel. Z′ resonances with masses below 2.26 TeV are excluded by this statistical combination.

Figure 3 (bottom) shows the comparison and combination of the results obtained in the 8 and

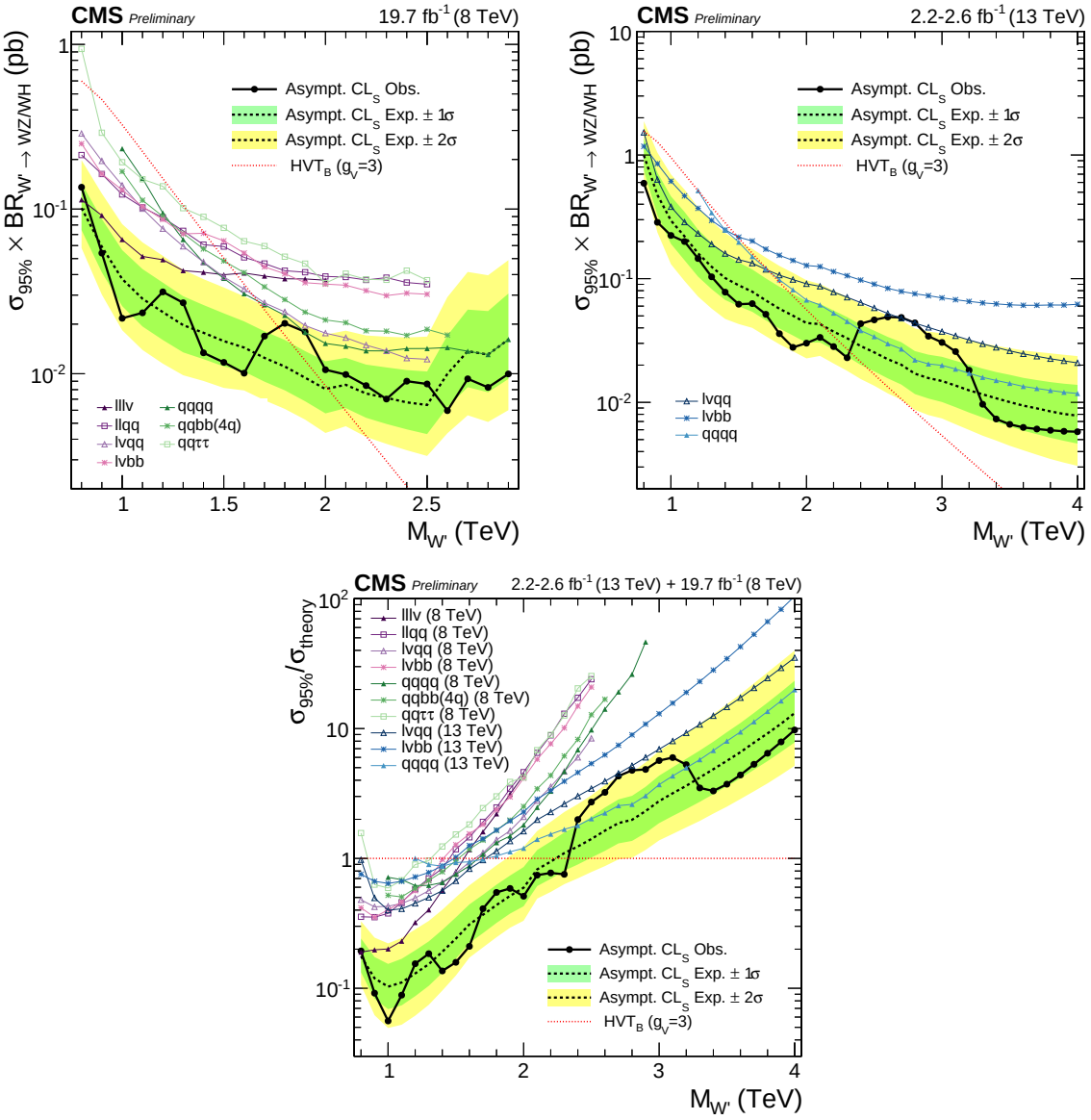

Figure 1: (top left) Observed (black solid) and expected (black dashed) exclusion limits at 95% CL on $\sigma(\mathrm{pp} \to \mathrm{W}' \to \mathrm{WZ/WH})$ as a function of the resonance mass obtained by combining the 8 TeV diboson searches. The curve corresponding to the cross sections predicted by the HVT model B is overlaid. (top right) Observed (black solid) and expected (black dashed) exclusion limits at 95% CL on $\sigma(\mathrm{pp} \to \mathrm{W}' \to \mathrm{WZ/WH})$ as a function of the resonance mass obtained by combining the 13 TeV diboson searches. The curve corresponding to the cross sections predicted by the HVT model B is overlaid. (bottom) Exclusion limits at 95% CL on the signal strength as a function of the resonance mass obtained by combining the 8 and 13 TeV diboson searches. In each of the three plots the different colored lines correspond to the searches entering the combination.

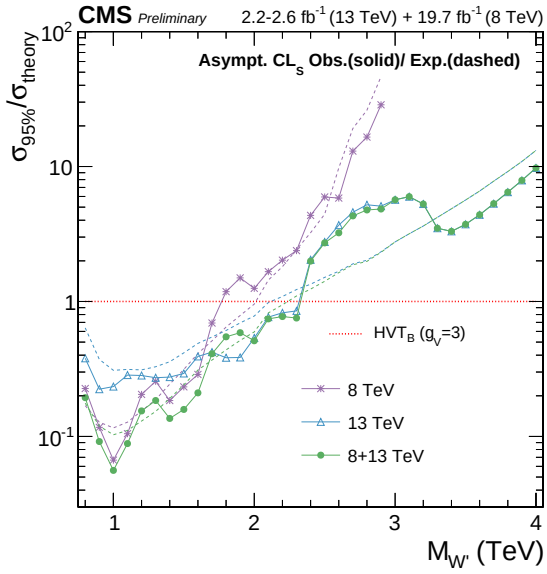

Figure 2: Comparison of the observed (solid) and expected (dashed) exclusion limits at 95% CL obtained by combining only 8 TeV or only 13 TeV searches to the results from the combination of all the 8 and 13 TeV results.

13 TeV searches. The 95% CL exclusion limits on the signal strength in the resonance mass range $0.8 < m_{W'} < 4$ TeV are shown. The $\ell\nu q\bar{q}$ channels dominate the sensitivity over the whole range, with 8 and 13 TeV analyses giving almost equal contributions for masses below 2 TeV. Above this value, the sensitivity is mainly driven by the 13 TeV analyses.

Figure 4 shows the comparison of the combination of 8 and 13 TeV results with the combination of only 8 TeV or only 13 TeV searches for the Z′ signal hypothesis. Under this signal hypothesis the sensitivities reached by the 8 and 13 TeV channels are similar at low resonance masses. Nevertheless, the combination improves the overall sensitivity by about 10–30% for resonance masses below 2 TeV. For higher values, the sensitivity reached by the 13 TeV searches supersedes the ones reached at 8 TeV. As for the W′ case the mass limit is not affected by the combination compared to what obtained from the 13 TeV searches, which supersedes the current most stringent limit of 1.4 TeV obtained from the 8 TeV diboson searches [32].

5.3 Limits on heavy vector triplet (W′ + Z′)

Figure 5 (top left) shows the comparison and combination of the results obtained in the 8 TeV VV and VH searches. The 95% CL exclusion limits on the sum of the W′ and Z′ production cross sections times the branching fraction of the corresponding decays to diboson in the resonance mass range $0.8 < m_{V'} < 2.9$ TeV (V′ =W′,Z′) are shown. At low masses ($\lesssim 1.3$ TeV) all the channels have similar sensitivities with a slightly more important contribution from the $\ell\nu q\bar{q}$ and VH all-hadronic channels, which are the most sensitive over the whole mass range. With the combination, the sensitivity on the cross section is improved by up to 70% with respect to the most sensitive $\ell\nu q\bar{q}$ channel. A lower mass limit of 2.1 TeV is obtained, about 10% higher than the limit reached by the $\ell\nu q\bar{q}$ channel. The excluded mass range is more stringent than the (1.0–1.7) TeV range excluded by 8 TeV diboson searches under the triplet interpretation [11].

Figure 5 (top right) shows the comparison and combination of the results obtained in the 13 TeV VV and VH searches in the resonance mass range $0.8 < m_{V'} < 4$ TeV. The sensitivity at lower masses ($\lesssim 1.8$ TeV) is mainly driven by the $\ell\nu q\bar{q}$ channel, while at high masses it is dominated by the all-hadronic channel. This differs from what is observed for the 8 TeV case,

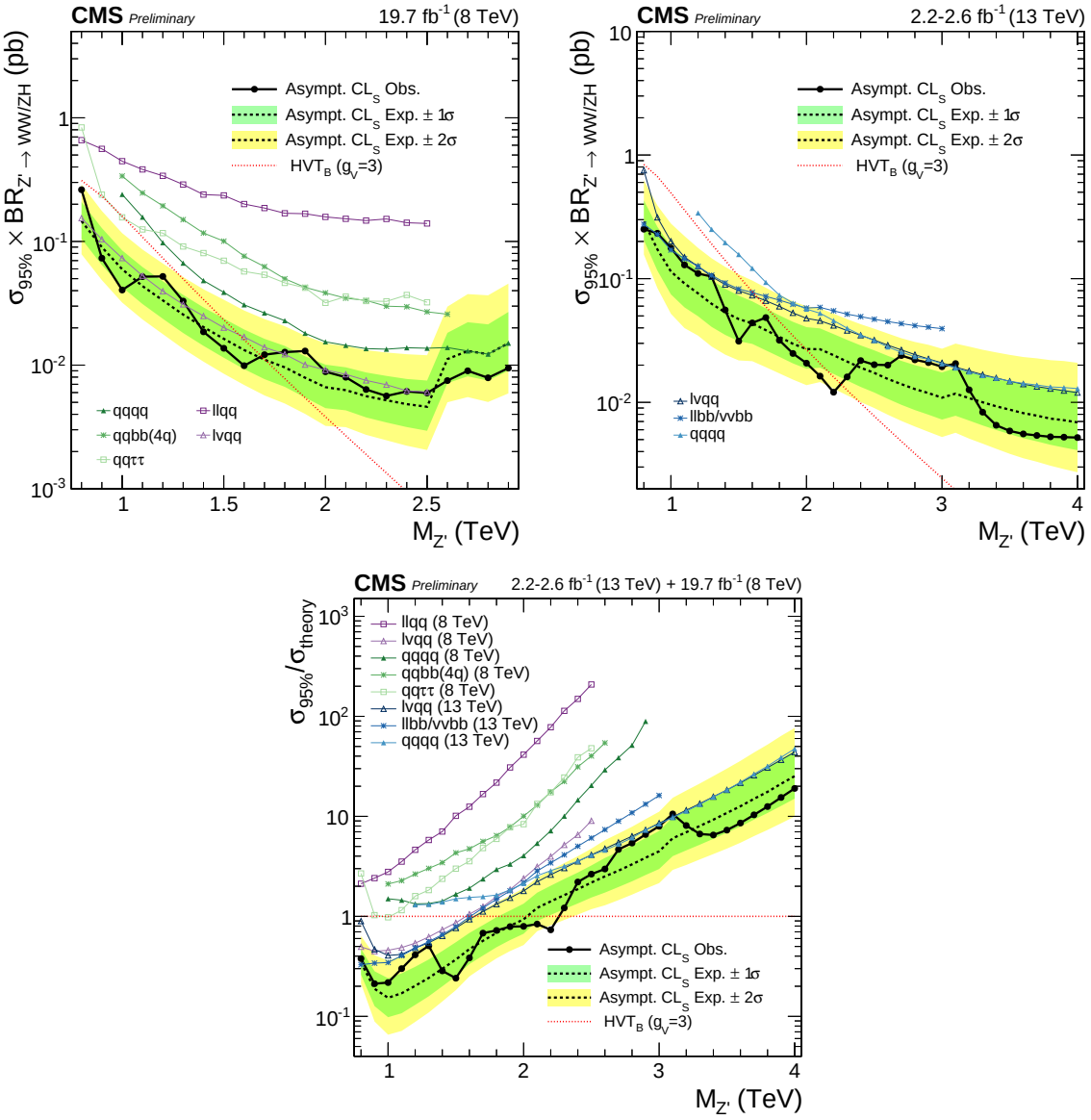

Figure 3: (top left) Observed (black solid) and expected (black dashed) exclusion limits at 95% CL on $\sigma(\mathrm{pp} \to \mathrm{Z}' \to \mathrm{WW/ZH})$ as a function of the resonance mass obtained by combining the 8 TeV diboson searches. The curve corresponding to the cross sections predicted by the HVT model B is overlaid. (top right) Observed (black solid) and expected (black dashed) exclusion limits at 95% CL on $\sigma(\mathrm{pp} \to \mathrm{Z}' \to \mathrm{WW/ZH})$ as a function of the resonance mass obtained by combining the 13 TeV diboson searches. The curve corresponding to the cross sections predicted by the HVT model B is overlaid. (bottom) Exclusion limits at 95% CL on the signal strength as a function of the resonance mass obtained by combining the 8 and 13 TeV diboson searches. In each of the three plots the different colored lines correspond to the searches entering the combination.

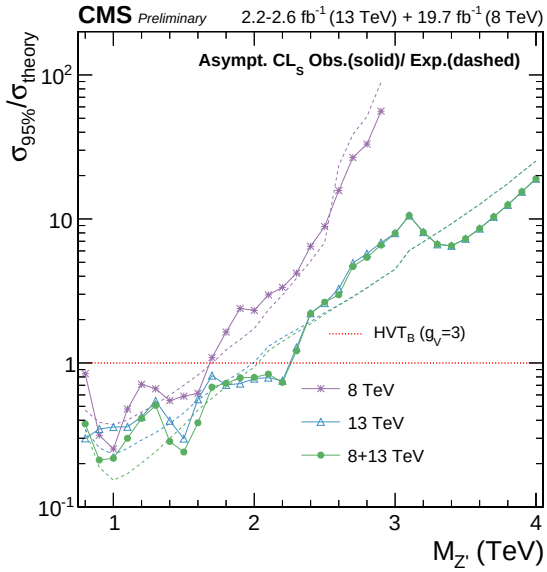

Figure 4: Comparison of the observed (solid) and expected (dashed) exclusion limits at 95% CL obtained by combining only 8 TeV or only 13 TeV searches to the results from the combination of all the 8 and 13 TeV results.

where the $\ell\nu q\bar{q}$ channel is the most sensitive over the whole range. With the combination, the sensitivity is improved by up to 40% both at low and high masses with respect to the most sensitive channel in the range. A lower mass limit of 2.38 TeV is obtained, about 12% higher than the limit obtained combining the 8 TeV searches.

Figure 5 (bottom) shows the comparison and combination of the results obtained in the 8 and 13 TeV searches. The 95% CL exclusion limits on the signal strength in the resonance mass range $0.8 < m_{W'} < 4$ TeV are shown. The $\ell\nu q\bar{q}$ channels dominate the sensitivity over the whole range together with the VH all-hadronic channel for masses below 2 TeV. Above this value, the sensitivity is mainly driven by the 13 TeV analyses. With the combination, a lower mass limit of 2.39 TeV is obtained, comparable to the value obtained combining only 13 TeV searches.

Figure 6 shows the comparison of the combination of 8 and 13 TeV results with the combination of only 8 TeV or only 13 TeV searches for the triplet hypothesis. For resonance masses below 2 TeV, the sensitivity is improved by 20–50% with respect to the 13 TeV combination and by 10–30% with respect to the 8 TeV combination. For masses above 2 TeV, the 8 TeV channels do not add any significant contribution. As for the W′ and Z′ cases, the observed mass limit of 2.39 TeV obtained combining 8 and 13 TeV searches is determined by the 13 TeV channels and it is the most stringent to date in the context of the HVT model in the B scenario.

In Fig. 7, a scan of the coupling parameters and the corresponding observed 95% CL exclusion contours in the HVT model from the combination of the 8 and 13 TeV analyses are shown. The parameters are defined as $g_V c_H$ and $g^2 c_F / g_V$, in terms of the coupling strengths (Section 2.1) of the new resonance to the Higgs boson and to fermions. The range of the scan is limited by the assumption that the new resonance is narrow. A contour is overlaid, representing the region where the theoretical width is larger than the experimental resolution of the searches, and hence where the narrow-resonance assumption is not satisfied. This contour is defined by a predicted resonance width of 7%, corresponding to the largest resonance mass resolution of the considered searches.

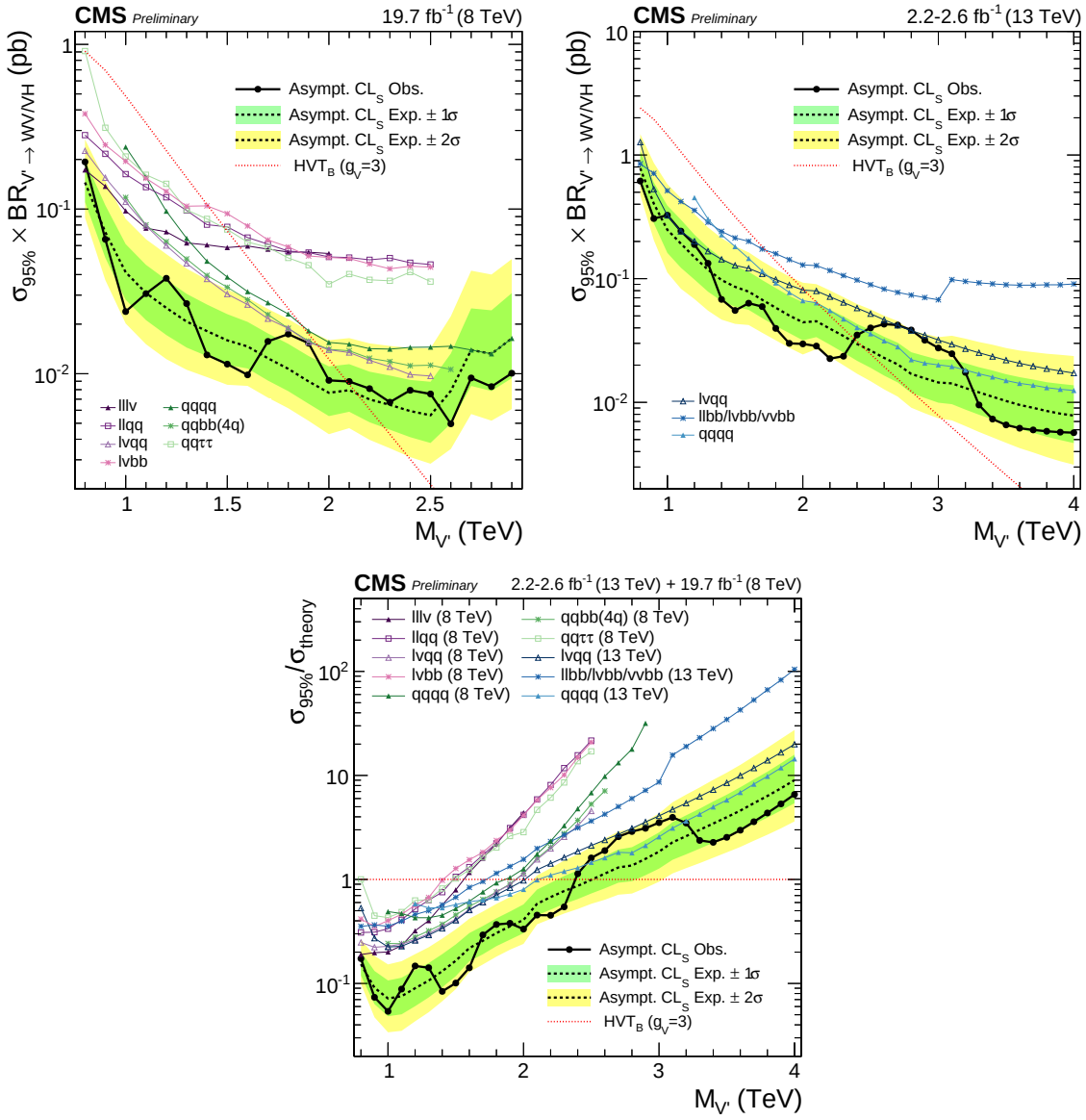

Figure 5: (top left) Observed (black solid) and expected (black dashed) exclusion limits at 95% CL on $\sigma(\mathrm{pp} \to \mathrm{V}' \to \mathrm{WV/VH})$ (V′ =W′,Z′ and V=W,Z) as a function of the resonance mass obtained by combining the 8 TeV diboson searches. The curve corresponding to the cross sections predicted by the HVT model B is overlaid. (top right) Observed (black solid) and expected (black dashed) exclusion limits at 95% CL on $\sigma(\mathrm{pp} \to \mathrm{V}' \to \mathrm{WV/VH})$ as a function of the resonance mass obtained by combining the 13 TeV diboson searches. The curve corresponding to the cross sections predicted by the HVT model B is overlaid. (bottom) Exclusion limits at 95% CL on the signal strength as a function of the resonance mass obtained by combining the 8 and 13 TeV diboson searches. In all the three plots the different colored lines correspond to the searches entering the combination.

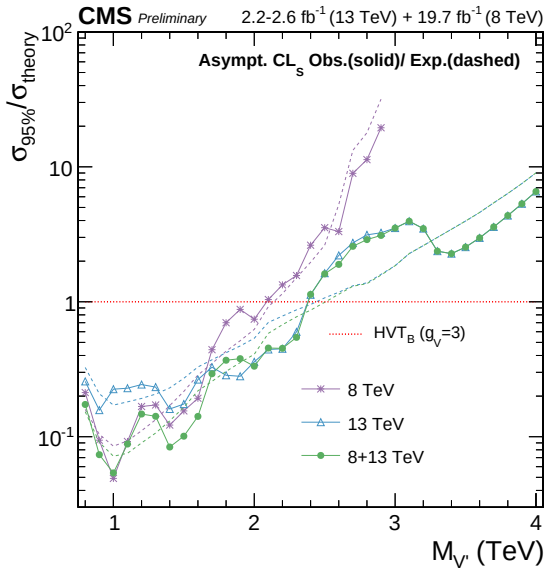

Figure 6: Comparison of the observed (solid) and expected (dashed) exclusion limits at 95% CL obtained by combining only 8 TeV or only 13 TeV searches to the results from the combination of all the 8 and 13 TeV results.

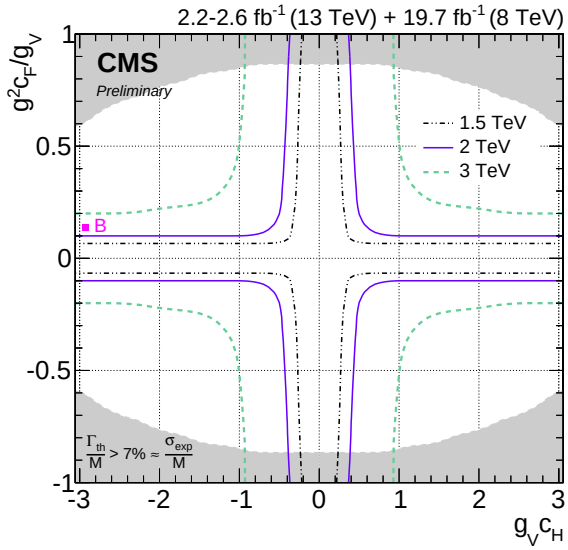

Figure 7: Exclusion regions in the plane of the HVT-model couplings ($g_V c_H$, $g^2 c_F / g_V$) for three resonance masses, 1.5, 2, and 3 TeV, where g denotes the weak gauge coupling. The point B of the benchmark model used in the analysis is also shown. The boundaries of the regions outside these lines are excluded by this search are indicated by the solid and dashed lines. The areas indicated by the solid shading correspond to regions where the resonance width is predicted to be more than 7% of the resonance mass and the narrow-resonance assumption is not satisfied.

5.4 Limits on Bulk Graviton

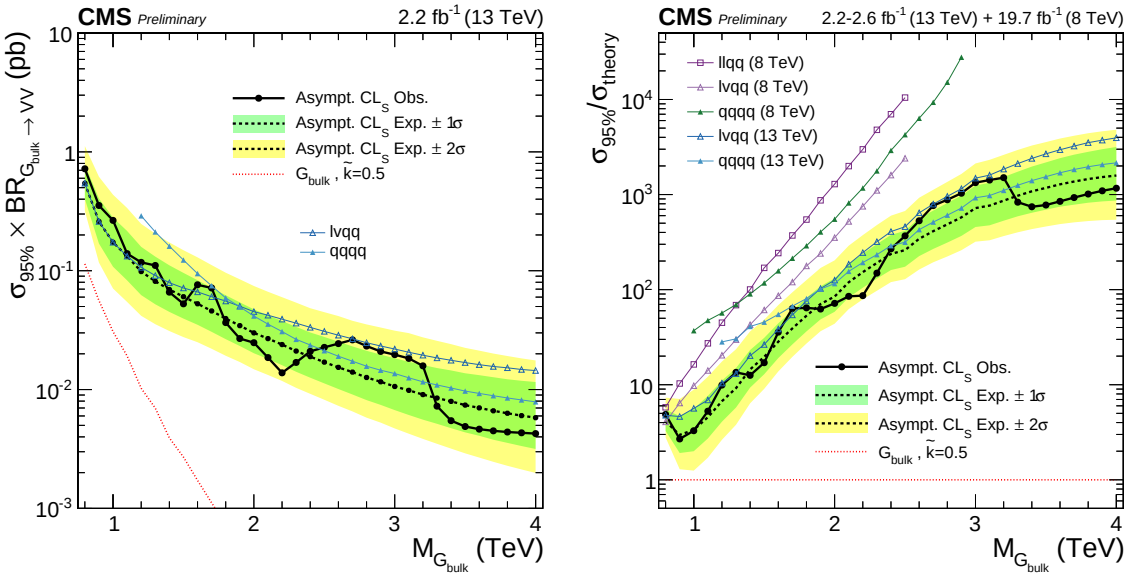

Figure 8: (left) Observed (black solid) and expected (black dashed) exclusion limits at 95% CL on $\sigma(\mathrm{pp} \to \mathrm{G_{bulk}} \to \mathrm{VV})$ (V=W,Z) as a function of the resonance mass obtained by combining the 13 TeV diboson searches. The curve corresponding to the cross sections predicted by bulk graviton model is overlaid. (right) Exclusion limits at 95% CL on the signal strength as a function of the resonance mass obtained by combining the 8 and 13 TeV diboson searches. In all the three plots the different colored lines correspond to the searches entering the combination.

Figure 8 (left) shows the comparison and combination of the results obtained in the 13 TeV VV searches in the resonance mass range $0.8 < m_{\mathrm{G}} < 4$ TeV. The 95% CL exclusion limits on the bulk graviton production cross section times the branching fraction to WW and ZZ obtained in the 13 TeV VV searches in the resonance mass range $0.8 < m_{\mathrm{G}} < 4$ TeV are shown. The sensitivity at lower masses ($\lesssim 1.8$ TeV) is mainly driven by the $\ell\nu\mathrm{q\bar{q}}$ channel, while at high masses it is dominated by the dijet channel. The limits are compared with the cross section times the branching fraction to WW for a bulk graviton with $k/\bar{M}_{Pl} = 0.5$. The sensitivity reached by the combination is not enough to exclude a range of masses in this particular model; however cross sections are excluded in the range [0.004–0.7] pb. This limit is improved with the combination by up to 40% both at low and high masses with respect to the most sensitive channel in the range.

Figure 8 (right) shows the comparison and combination of the results obtained in the 8 and 13 TeV VV searches. The 95% CL exclusion limits on the signal strength in the resonance mass range $0.8 < m_{\mathrm{G}} < 4$ TeV are shown. At a resonance mass of 2 TeV the sensitivity on the cross section reached by the 13 TeV searches supersedes the 8 TeV searches by factors of 2.1 and 3.6 for the $\ell\nu\mathrm{q\bar{q}}$ and $\mathrm{q\bar{q}q\bar{q}}$ channel, respectively. The combination yields the most stringent signal strength limits on a narrow bulk graviton resonances to date in the mass range from 0.8 to 4 TeV.

Figure 9 shows the comparison of the combination of 8 and 13 TeV results with the combination of only 8 TeV or only 13 TeV searches for the bulk graviton signal hypothesis. Under this signal hypothesis, the sensitivity reached by the 13 TeV searches supersedes the 8 TeV combination by 10–50% down to very low resonance masses (0.9 TeV). Hence, the contribution given by 8 TeV channels is less significant with respect to the spin-1 resonance hypotheses. Nevertheless, with the combination the sensitivity is improved by 10–40% for resonance masses below 1.6 TeV.

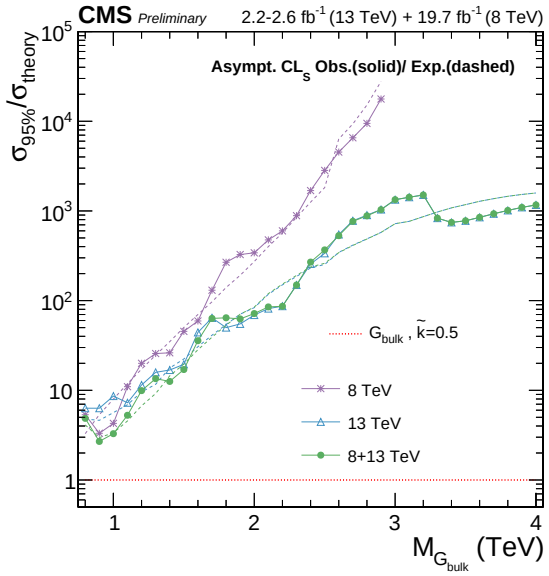

Figure 9: Comparison of the observed (solid) and expected (dashed) exclusion limits at 95% CL obtained by combining only 8 TeV or only 13 TeV searches to the results from the combination of all the 8 and 13 TeV results.

5.5 Significance at 2 TeV

ATLAS reported an excess in the all-hadronic VV search in the $q\bar{q}q\bar{q}$ final state corresponding to a local significance of 3.4σ for a W′ resonance with a mass of 2 TeV [15]. CMS reported a local deviation of 2.2σ in the semi-leptonic WH $\rightarrow \ell\nu b\bar{b}$ search for a W′ resonance with a mass of 1.8 TeV [13]. We evaluate the combined significance of the 8 and 13 TeV CMS searches in the range 1.8–2.0 TeV in Tables 5–7. Combining all 8 TeV VH searches in the W′ hypothesis, the local significance of the excess at 1.8 TeV is slightly reduced to 2.1σ. Combining all 8 TeV VV/VH searches in the W′ hypothesis, it is increased back to 2.2σ. However, in combination with the 13 TeV VV/VH searches in the W′ hypothesis, the overall significance at 1.8 TeV is reduced to 0.9σ. This remains the largest significance for the overall combination of 8+13 TeV searches considering all signal hypothesis over the mass range 1.8–2.0 TeV, thus not supporting the excesses observed in the two individual channels in 8 TeV data.

Table 5: Statistical significance of excesses observed at 1.8 TeV in the various searches, expressed in standard deviations.

Combination	W′	Z′	HVT (W′ +Z′)	G_{bulk}
VV 13 TeV	0.00	0.10	0.00	0.00
VV+VH 13 TeV	0.00	0.00	0.00	-
VV 8 TeV	1.22	0.56	1.03	1.61
VV 8+13 TeV	0.20	0.46	0.33	0.35
VH 8 TeV	2.05	0.56	1.79	-
VV+VH 8 TeV	2.22	0.77	1.95	-
VV+VH 8+13 TeV	0.86	0.00	0.83	-

6 Conclusions

The statistical combination of searches for massive resonances decaying to WW, ZZ, WZ, WH, and ZH boson pairs has been presented. The considered searches are based on pp collision data

Table 6: Statistical significance of excesses observed at 1.9 TeV in the various searches, expressed in standard deviations.

Combination	W′	Z′	HVT (W′ +Z′)	G_{bulk}
VV 13 TeV	0.00	0.05	0.00	0.00
VV+VH 13 TeV	0.00	0.00	0.00	-
VV 8 TeV	1.20	0.46	0.91	1.05
VV 8+13 TeV	0.00	0.30	0.00	0.00
VH 8 TeV	2.17	1.41	1.78	-
VV+VH 8 TeV	2.32	1.02	1.89	-
VV+VH 8+13 TeV	0.33	0.00	0.20	-

Table 7: Statistical significance of excesses observed at 2 TeV in the various searches, expressed in standard deviations.

Combination	W′	Z′	HVT (W′ +Z′)	G_{bulk}
VV 13 TeV	0.00	0.07	0.00	0.00
VV+VH 13 TeV	0.00	0.00	0.00	-
VV 8 TeV	0.77	0.75	0.76	0.44
VV 8+13 TeV	0.23	0.45	0.29	0.06
VH 8 TeV	0.00	0.00	0.00	-
VV+VH 8 TeV	0.58	0.60	0.48	-
VV+VH 8+13 TeV	0.00	0.00	0.00	-

collected by the CMS experiment at a centre-of-mass energy of 8 and 13 TeV, corresponding to an integrated luminosity of 19.7 fb^{-1} and 2.2– 2.6 fb^{-1}, respectively. The results are interpreted in the context of heavy vector singlet and triplet models predicting a W′ and a Z′ decaying to WZ, WH, WW, and ZH and a model with a "bulk" graviton that decays into WW and ZZ. The combination yields the most stringent resonance mass limits to date on W′ and Z′ singlets at 2.3 TeV and 1.8 TeV, respectively, and on a heavy vector triplet at 2.4 TeV. The combination also yields the most stringent cross section limits on a narrow bulk graviton resonance to date in the mass range from 0.8 to 4 TeV. Finally, the combined significance of a potential resonances at 1.8–2.0 TeV is evaluated and found to be 0.9σ for the hypothesis of a W′ that yields the highest significance among all considered signal hypotheses.

References

[1] L. Randall and R. Sundrum, "A Large mass hierarchy from a small extra dimension", *Phys. Rev. Lett.* **83** (1999) 3370, doi:10.1103/PhysRevLett.83.3370, arXiv:hep-ph/9905221.

[2] L. Randall and R. Sundrum, "An Alternative to compactification", *Phys. Rev. Lett.* **83** (1999) 4690, doi:10.1103/PhysRevLett.83.4690, arXiv:hep-th/9906064.

[3] B. Bellazzini, C. Csáki, and J. Serra, "Composite Higgses", *Eur. Phys. J. C* **74** (2014) 2766, doi:10.1140/epjc/s10052-014-2766-x, arXiv:1401.2457.

[4] R. Contino, D. Marzocca, D. Pappadopulo, and R. Rattazzi, "On the effect of resonances in composite Higgs phenomenology", *JHEP* **10** (2011) 081, doi:10.1007/JHEP10(2011)081, arXiv:1109.1570.

[5] D. Marzocca, M. Serone, and J. Shu, "General composite Higgs models", *JHEP* **08** (2012) 013, doi:10.1007/JHEP08(2012)013, arXiv:1205.0770.

[6] D. Greco and D. Liu, "Hunting composite vector resonances at the LHC: naturalness facing data", *JHEP* **12** (2014) 126, doi:10.1007/JHEP12(2014)126, arXiv:1410.2883.

[7] CMS Collaboration, "Search for massive resonances decaying into pairs of boosted W and Z bosons at $\sqrt{s}$=13 TeV", CMS Physics Analysis Summary CMS-PAS-EXO-15-002, 2015.

[8] CMS Collaboration, "Search for heavy resonances decaying into a vector boson and a Higgs boson in the ($\ell\ell$, $\ell\nu$, $\nu\nu$) $\mathrm{b\bar{b}}$ final state", CMS Physics Analysis Summary CMS-PAS-B2G-16-003, 2016.

[9] CMS Collaboration, "Search for massive resonances decaying into pairs of boosted bosons in semi-leptonic final states at $\sqrt{s} = 8$ TeV", *JHEP* **08** (2014) 174, doi:10.1007/JHEP08(2014)174, arXiv:1405.3447.

[10] CMS Collaboration, "Search for massive resonances in dijet systems containing jets tagged as W or Z boson decays in pp collisions at $\sqrt{s}$ = 8 TeV", *JHEP* **08** (2014) 173, doi:10.1007/JHEP08(2014)173, arXiv:1405.1994.

[11] CMS Collaboration, "Search for a massive resonance decaying into a Higgs boson and a W or Z boson in hadronic final states in proton-proton collisions at $\sqrt{s} = 8$ TeV", *JHEP* **02** (2016) 145, doi:10.1007/JHEP02(2016)145, arXiv:1506.01443.

[12] CMS Collaboration, "Search for new resonances decaying via WZ to leptons in proton-proton collisions at $\sqrt{s} = 8$ TeV", *Phys. Lett. B* **740** (2015) 83, doi:10.1016/j.physletb.2014.11.026, arXiv:1407.3476.

[13] CMS Collaboration, "Search for massive WH resonances decaying into the $\ell\nu\mathrm{b\bar{b}}$ final state at $\sqrt{s} = 8$ TeV", *Eur. Phys. J. C* **76** (2016) 237, doi:10.1140/epjc/s10052-016-4067-z, arXiv:1601.06431.

[14] CMS Collaboration, "Search for Narrow High-Mass Resonances in Proton-Proton Collisions at $\sqrt{s}$ = 8 TeV Decaying to a Z and a Higgs Boson", *Phys. Lett. B* **748** (2015) 255, doi:10.1016/j.physletb.2015.07.011, arXiv:1502.04994.

[15] ATLAS Collaboration, "Search for high-mass diboson resonances with boson-tagged jets in proton-proton collisions at $\sqrt{s} = 8$ TeV with the ATLAS detector", *JHEP* **12** (2015) 055, doi:10.1007/JHEP12(2015)055, arXiv:1506.00962.

[16] K. Agashe, H. Davoudiasl, G. Perez, and A. Soni, "Warped Gravitons at the LHC and Beyond", *Phys. Rev. D* **76** (2007) 036006, doi:10.1103/PhysRevD.76.036006, arXiv:hep-ph/0701186.

[17] A. L. Fitzpatrick, J. Kaplan, L. Randall, and L.-T. Wang, "Searching for the Kaluza-Klein Graviton in Bulk RS Models", *JHEP* **09** (2007) 013, doi:10.1088/1126-6708/2007/09/013, arXiv:hep-ph/0701150.

[18] O. Antipin, D. Atwood, and A. Soni, "Search for RS gravitons via $W_L W_L$ decays", *Phys. Lett. B* **666** (2008) 155, doi:10.1016/j.physletb.2008.07.009, arXiv:0711.3175.

[19] D. Pappadopulo, A. Thamm, R. Torre, and A. Wulzer, "Heavy Vector Triplets: Bridging Theory and Data", *JHEP* **09** (2014) 060, doi:10.1007/JHEP09(2014)060, arXiv:1402.4431.

[20] M. Schmaltz and D. Tucker-Smith, "Little Higgs review", *Ann. Rev. Nucl. Part. Sci.* **55** (2005) 229, doi:10.1146/annurev.nucl.55.090704.151502, arXiv:hep-ph/0502182.

[21] N. Arkani-Hamed, A. Cohen, E. Katz, and A. Nelson, "The Littlest Higgs", *JHEP* **07** (2002) 034, doi:10.1088/1126-6708/2002/07/034, arXiv:hep-ph/0206021.

[22] G. Altarelli, B. Mele, and M. Ruiz-Altaba, "Searching for new heavy vector bosons in $p\bar{p}$ colliders", *Zeitschrift für Physik C Particles and Fields* **45** (1989) 109, doi:10.1007/BF01556677.

[23] CMS Collaboration, "Search for physics beyond the standard model in final states with a lepton and missing transverse energy in proton-proton collisions at $\sqrt{s} = 8$ TeV", *Phys. Rev. D* **91** (2015) 092005, doi:10.1103/PhysRevD.91.092005, arXiv:1408.2745.

[24] ATLAS Collaboration, "Search for new particles in events with one lepton and missing transverse momentum in pp collisions at $\sqrt{s} = 8$ TeV with the ATLAS detector", *JHEP* **09** (2014) 037, doi:10.1007/JHEP09(2014)037, arXiv:1407.7494.

[25] CMS Collaboration, "Search for SSM W' production, in the lepton+MET final state at a center-of-mass energy of 13 TeV", CMS Physics Analysis Summary CMS-PAS-EXO-15-006, 2015.

[26] ATLAS Collaboration, "Combination of searches for WW, WZ, and ZZ resonances in pp collisions at $\sqrt{s} = 8$ TeV with the ATLAS detector", *Phys. Lett. B* **755** (2016) 285, doi:10.1016/j.physletb.2016.02.015, arXiv:1512.05099.

[27] ATLAS Collaboration, "Search for production of WW/WZ resonances decaying to a lepton, neutrino and jets in pp collisions at $\sqrt{s} = 8$ TeV with the ATLAS detector", *Eur. Phys. J. C* **75** (2015) 209, doi:10.1140/epjc/s10052-015-3593-4, 10.1140/epjc/s10052-015-3425-6, arXiv:1503.04677. [Erratum: *Eur. Phys. J. C* 75 (2015) 370].

[28] ATLAS Collaboration, "Search for WZ resonances in the fully leptonic channel using pp collisions at $\sqrt{s}$ = 8 TeV with the ATLAS detector", *Phys. Lett. B* **737** (2014) 223, doi:10.1016/j.physletb.2014.08.039, arXiv:1406.4456.

[29] CMS Collaboration, "Search for physics beyond the standard model in dilepton mass spectra in proton-proton collisions at $\sqrt{s} = 8$ TeV", *JHEP* **04** (2015) 025, doi:10.1007/JHEP04(2015)025, arXiv:1412.6302.

[30] ATLAS Collaboration, "Search for high-mass dilepton resonances in pp collisions at $\sqrt{s} = 8$TeV with the ATLAS detector", *Phys. Rev. D* **90** (2014) 052005, doi:10.1103/PhysRevD.90.052005, arXiv:1405.4123.

[31] CMS Collaboration, "Search for a Narrow Resonance Produced in 13 TeV pp Collisions Decaying to Electron Pair or Muon Pair Final States", CMS Physics Analysis Summary CMS-PAS-EXO-15-005, 2015.

[32] ATLAS Collaboration, "Search for a new resonance decaying to a W or Z boson and a Higgs boson in the $\ell\ell/\ell\nu/\nu\nu + b\bar{b}$ final states with the ATLAS detector", *Eur. Phys. J. C* **75** (2015) 263, doi:10.1140/epjc/s10052-015-3474-x, arXiv:1503.08089.

[33] M. Wobisch and T. Wengler, "Hadronization corrections to jet cross-sections in deep inelastic scattering", in *Monte Carlo generators for HERA physics. Proceedings, Workshop, Hamburg, Germany, 1998-1999*. 1998. arXiv:hep-ph/9907280.

[34] M. Cacciari, G. P. Salam, and G. Soyez, "The anti-k_t jet clustering algorithm", *JHEP* **04** (2008) 063, doi:10.1088/1126-6708/2008/04/063, arXiv:0802.1189.

[35] S. D. Ellis, C. K. Vermilion, and J. R. Walsh, "Techniques for improved heavy particle searches with jet substructure", *Phys. Rev. D* **80** (2009) 051501, doi:10.1103/PhysRevD.80.051501, arXiv:0903.5081.

[36] S. D. Ellis, C. K. Vermilion, and J. R. Walsh, "Recombination Algorithms and Jet Substructure: Pruning as a Tool for Heavy Particle Searches", *Phys. Rev. D* **81** (2010) 094023, doi:10.1103/PhysRevD.81.094023, arXiv:0912.0033.

[37] J. Thaler and K. Van Tilburg, "Identifying Boosted Objects with N-subjettiness", *JHEP* **03** (2011) 015, doi:10.1007/JHEP03(2011)015, arXiv:1011.2268.

[38] R. D. Ball et al., "Impact of Heavy Quark Masses on Parton Distributions and LHC Phenomenology", *Nucl. Phys. B* **849** (2011) 296, doi:10.1016/j.nuclphysb.2011.03.021, arXiv:1101.1300.

[39] M. Cacciari et al., "The $t\bar{t}$ cross-section at 1.8-TeV and 1.96-TeV: A Study of the systematics due to parton densities and scale dependence", *JHEP* **04** (2004) 068, doi:10.1088/1126-6708/2004/04/068, arXiv:hep-ph/0303085.

[40] S. Catani, D. de Florian, M. Grazzini, and P. Nason, "Soft gluon resummation for Higgs boson production at hadron colliders", *JHEP* **07** (2003) 028, doi:10.1088/1126-6708/2003/07/028, arXiv:hep-ph/0306211.

[41] G. Cowan, K. Cranmer, E. Gross, and O. Vitells, "Asymptotic formulae for likelihood-based tests of new physics", *Eur. Phys. J. C* **71** (2011) 1554, doi:10.1140/epjc/s10052-011-1554-0, 10.1140/epjc/s10052-013-2501-z, arXiv:1007.1727.

[42] A. L. Read, "Presentation of search results: The CL_s technique", *J. Phys. G* **28** (2002) 2693, doi:10.1088/0954-3899/28/10/313.

[43] T. Junk, "Confidence level computation for combining searches with small statistics", *Nucl. Instrum. Meth. A* **434** (1999) 435, doi:10.1016/S0168-9002(99)00498-2, arXiv:hep-ex/9902006.

[44] ATLAS and CMS Collaborations, LHC Higgs Combination Group, "Procedure for the LHC Higgs boson search combination in Summer 2011", Technical Report ATL-PHYS-PUB 2011-11, CMS NOTE 2011/005, 2011.